

# Production cross sections for the heaviest nuclei in complete fusion reactions induced by heavy ions

R.N. Sagaidak<sup>a</sup>

Flerov Laboratory of Nuclear Reactions, Joint Institute for Nuclear Research, Dubna 141980, Russia

Received 14 November 2006 / Received in final form 7 March 2007

Published online 16 May 2007 – © EDP Sciences, Società Italiana di Fisica, Springer-Verlag 2007

**Abstract.** Production of the heaviest nuclei in complete fusion reactions induced by heavy ions has been considered in a systematic way in the framework of the conventional barrier passing model coupled with the statistical model. Available data on excitation functions for fission and production of evaporation residues (ER) in very asymmetric combinations induced by ions lighter than Ne on actinide target nuclei are described rather well in the framework of these models. The data allow one to adjust model parameters and to reveal the quasi-fission effect caused by the interaction with deformed target nuclei, which is manifested in the suppression of the ER production at sub-barrier energies. For reactions induced by Mg and heavier projectiles, quasi-fission is starting to suppress fusion (ER production) at energies above the Coulomb barrier. One has to introduce empirically the quantity of the fusion probability  $P_{\text{fus}}$  to reproduce the ER excitation functions in the framework of the conventional approach. The exponential dependence of  $P_{\text{fus}}$  on the combined fissility parameter (a similar parameter that was introduced for the extra-push energy scaling) was found in search for scaling for the  $P_{\text{fus}}$  values resulting from the data analysis.

**PACS.** 25.70.Gh Compound nucleus – 25.85.-w Fission reactions

## 1 Introduction

Synthesis of the heaviest nuclei in complete fusion reactions with heavy ions still remains an attractive field of activity after about 40 years history of these researches. One can designate three main directions in using the reactions of synthesis, which are traced in last years. (1) “Cold fusion” reactions of medium heavy ions (from  $^{40}\text{Ar}$  to  $^{86}\text{Kr}$ ) with Pb and Bi target nuclei, which were discovered by Oganessian in Dubna [1] and then were continued to use by Münzenberg, Hofmann et al. at GSI [2], and later by Morita et al. at RIKEN [3] for the synthesis of neutron deficient nuclei with  $104 \leq Z \leq 113$ . (2) “Hot fusion” reactions of relatively light heavy ions (from  $^{18}\text{O}$  to  $^{34}\text{S}$ ) with actinide target nuclei, which are mainly used now for chemical studies of the heaviest elements ( $Z \leq 108$ ) [4]. (3) Reactions of  $^{48}\text{Ca}$  with actinide target nuclei that are used by Oganessian et al. for the synthesis of the heaviest nuclei with  $112 \leq Z \leq 118$  [5], the nearest ones to the island of stability of superheavy elements (SHE) predicted by theory.

Intensive studies of the mechanisms of complete fusion were undertaken in the last 25 years. Studies of fission [6–8] and ER production [9–11] in reactions leading to very heavy composite systems, make it evident that the growing quasi-fission (QF) effect leads to a rapid decrease in the fusion probability and consequently to the

decrease in production cross section of the heaviest elements as their atomic number is increased. Such dependence is clear cut in the case of “cold fusion” reactions [2]. A number of models were developed to understand the mechanism of fusion leading to SHE and to predict their production cross sections. Some of them are based on the di-nuclear system concept (see, e.g., recent results of calculations in [12,13] and references therein), another one uses a similar two-center model approach [14]. Significant contributions to the field were done in the recent works [15,16].

In the present work an attempt is embarked on the systematic analysis of the ER and fission excitation functions obtained in reactions leading to  $Z \geq 98$  with the potential barrier-passing (BP) model describing capture/fusion cross sections obtained in experiments, and with the standard statistical model (SSM) describing the de-excitation of the compound nucleus (CN) resulting from complete fusion of the projectile and target nuclei. Both models are incorporated into the popular HIVAP code [17]. An idea of such analysis is to try to describe the ER and fission excitation functions for a specific combination simultaneously, bearing in mind that in the case of strongly fissile compound nuclei, for the BP/capture, fusion and CN-fission cross sections take place the relations  $\sigma_{\text{bp}} \equiv \sigma_{\text{fus}} \simeq \sigma_{\text{CN-fis}}$ . This is the case when the fusion probability  $P_{\text{fus}} = 1$ , i.e., according to the model, all the partial waves passing through the potential barrier lead to complete

<sup>a</sup> e-mail: sagaidak@nrmail.jinr.ru

fusion (CN formation). Such situation usually corresponds to very asymmetric projectile-target combinations when QF is negligible [10,11]. Going to heavier compound nuclei or/and to more massive projectiles (more symmetric combinations), when QF becomes a dominating effect ( $\sigma_{\text{fus}} < \sigma_{\text{cap}}$ ), i.e., in calculations  $\sigma_{\text{fus}} < \sigma_{\text{bp}}$  and one has  $P_{\text{fus}} < 1$  [10,11,18]. Since in the calculations with HIVAP, it is implied that  $P_{\text{fus}} = 1$ , one can derive an actual  $P_{\text{fus}}$  value comparing the ER and fission cross sections predicted by the model with those obtained in an experiment. Thus with this approach one can find a point when QF starts to be important and to suppress fusion (ER production). A systematic behavior of the  $P_{\text{fus}}$  derived with such analysis can help to predict production cross sections for unknown nuclei synthesized in different projectile-target combinations. Bearing in mind that production cross sections for the heaviest unknown nuclei are in the picobarn region and even below, reliable estimates could be useful from the point view of planning of future experiments.

## 2 “Hot fusion” reactions

For the derivation of the fusion probability it is convenient to consider combinations with a different entrance-channel mass-asymmetry, which lead to the same CN, as was done in the analysis of reactions leading to the compound nuclei in the region from Pb to Pa [9–11,18]. In that case one can extract the fusion probability value resulting from the difference in the ER production cross sections observed in very asymmetric and less asymmetric reactions. Essentially the same parameter values of SSM describing the de-excitation of the same CN should be used in that case. The expression of Reisdorf [17] was chosen for the macroscopic level density parameters  $\tilde{a}_f$  and  $\tilde{a}_\nu$  in the fission and evaporation channels, respectively. The scaling factor  $k_f$  at the rotating liquid drop (LD) fission barriers  $B_f^{\text{LD}}(L)$  [19] was used as a main fit parameter of SSM in the expression for fission barriers  $B_f(L) = k_f B_f^{\text{LD}}(L) - \Delta W_{\text{gs}}$ , where the shell correction energy  $\Delta W_{\text{gs}}$  is the difference between the empirical [20] and LD masses. In the case of reactions induced by  $^{48}\text{Ca}$  leading to compound nuclei close to the SHE region, where the empirical masses are not available, calculated masses [21] were used. The nuclear potential parameters of the BP model, such as the radius-parameter  $r_0 = 1.12$  fm and diffuseness  $d = 0.75$  fm, were fixed with the exception of the strength  $V_0$  and the barrier fluctuation determined by the radius-parameter fluctuation  $\sigma(r_0)/r_0$  in the exponential form of the potential [22]. Some variations of these parameters allowed one to achieve good agreement of the calculations with experimental data for fission and ER production at sub-barrier energies. Transmission coefficients were obtained using the WKB approximation. Note that for strongly fissile compound nuclei, the ER cross sections at energies well above the Coulomb (the nominal fusion barrier [23]) are weakly sensitive to the form of the nuclear potential and are mainly determined by the SSM parameters. Similar applications of HIVAP were used in [11,18], where

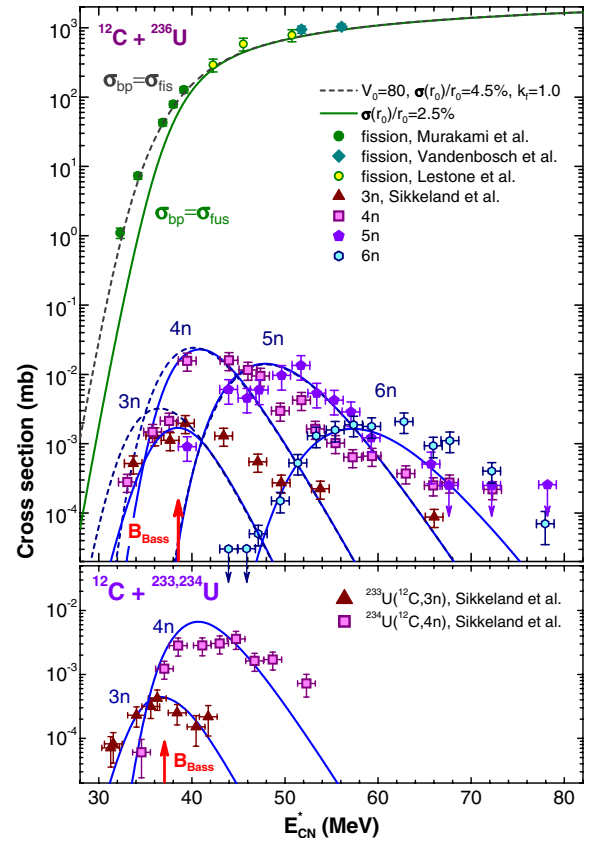


**Fig. 1.** (Color online) ER and fission cross sections obtained in  $^{12}\text{C} + \text{U}$  reactions [26,27] (symbols) in comparison to the calculations with HIVAP [17] (lines).

some additional information on the model can be found (see also [9,17,22,24]).

The available data on ER and fission excitation functions for the most asymmetric combinations leading to  $98 \leq Z_{\text{CN}} \leq 104$  were fitted assuming no fusion suppression ( $P_{\text{fus}} = 1$ ). The results are shown in Figures 1–3. As we see in Figures 1 and 2, fission excitation functions at sub-barrier energies are reproduced in the calculations with larger values of the barrier fluctuation parameter than those for ER. It means that fission events observed below the fusion barrier [23] belong mainly not to CN-fission (do not contribute to  $\sigma_{\text{fus}}$ ), but rather to QF, i.e., to the process that does not compete with the ER production in the CN decay. The QF character of fission cross sections at sub-barrier energies is in agreement with the results of the analysis of the fission-fragment angular anisotropy and can be caused by a strong deformation of the actinide target nuclei [25]. At energies above the barrier, the predictions of HIVAP correspond to fission and ER cross sections obtained in experiments. Note that the fitted LD fission barriers for Fm are about 20% higher than the nominal ones [19] required to describe excitation functions for the production of the relatively neutron-rich and neutron-deficient Fm isotopes (see Fig. 2). One should use a similar scaling of the LD fission barriers to describe the  $xn$  excitation functions for the production

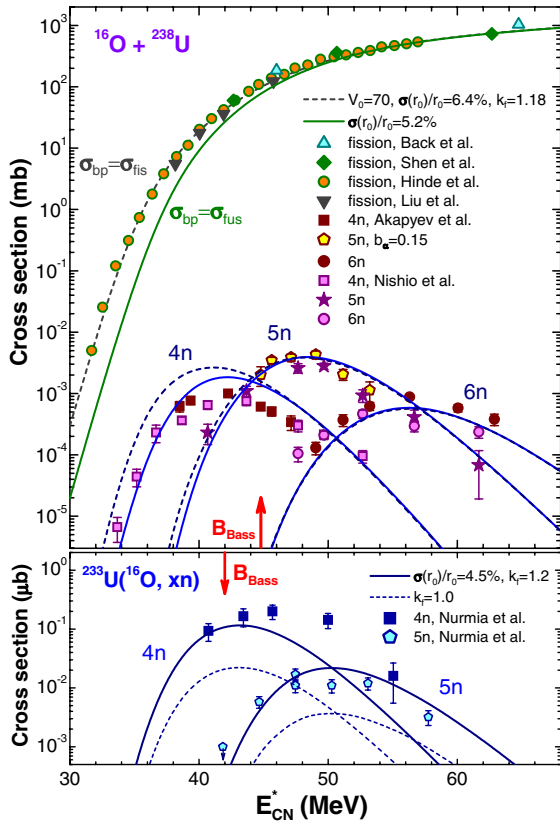


**Fig. 2.** (Color online) The same as in Figure 1, but for the  $^{16}\text{O} + ^{238}\text{U}$ ,  $^{233}\text{U}(^{16}\text{O}, xn)$  reactions [8,25,28–30]. The effect of 20% increase in  $k_f$  on the ER production cross section is shown (bottom panel).

of No isotopes in the  $^{12,13}\text{C} + ^{244,246,248}\text{Cm}$  reactions [31] and for Rf isotopes produced in very asymmetric combinations with  $^{15}\text{N}$  and  $^{16}\text{O}$  (see upper panels in Fig. 3). At the same time, applying this result to the data obtained in less asymmetric combinations with  $^{22}\text{Ne}$  and  $^{26}\text{Mg}$ , one has to introduce a 50% fusion probability in order to describe better the  $xn$  evaporation cross sections [32,33]. The value of  $P_{\text{fus}} = 0.5$  corresponds to the fusion cross sections deduced from the fission study in the  $^{26}\text{Mg} + ^{238}\text{U}$  reaction [8] (see right bottom panel in Fig. 3).

The results of the analysis of cross section data for the production of heavier nuclei are less unambiguous. Thus the data for the heaviest isotopes of Rf and Sg produced in the  $^{22}\text{Ne} + ^{244}\text{Pu}$ ,  $^{248}\text{Cm}$  reactions [4,33] can be reproduced with the same  $P_{\text{fus}}$  and  $k_f$  values as in the previous cases of the  $^{22}\text{Ne}$  and  $^{26}\text{Mg}$  reactions, and also with  $P_{\text{fus}} = 1$  and  $k_f = 1.15$  (using the same parameter values for the nuclear potential). Production cross sections of Db isotopes obtained in reactions with  $^{18}\text{O}$  and  $^{19}\text{F}$  (see the compilation in [34]) are also reproduced quite well with  $P_{\text{fus}} = 1$  and  $k_f = 1.2$ . So, one can state that QF may start to reduce the ER cross section at energies above the Coulomb barrier in reactions of  $^{22}\text{Ne}$  with actinide target nuclei. The analysis of the  $^{26}\text{Mg} + ^{248}\text{Cm}$  data leads to  $P_{\text{fus}} = 0.1$  at  $k_f = 1.0$ , which allows to reproduce  $xn$  evaporation cross sections [4]. Note that in this case a 20% vari-

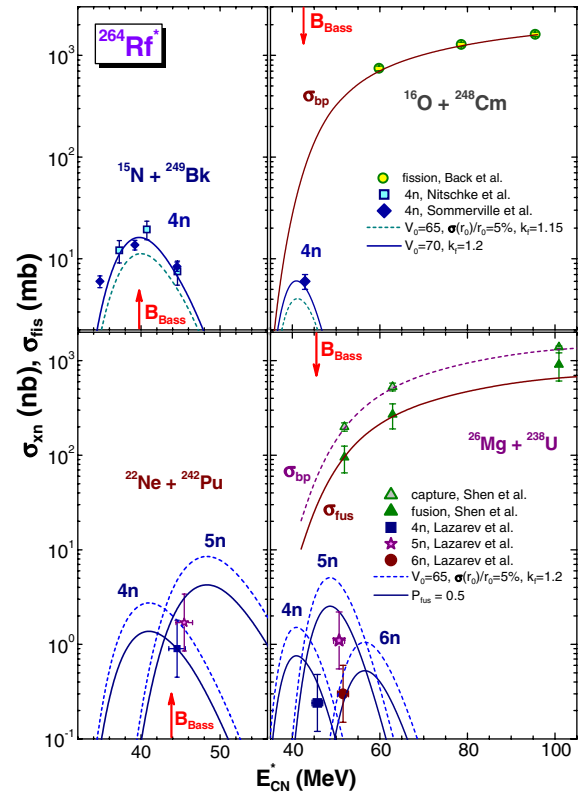


**Fig. 3.** (Color online) The same as in Figures 1 and 2, but for the cross sections obtained in reactions leading to  $^{264}\text{Rf}^*$  CN [7,8,32,33].  $P_{\text{fus}} < 1$  is introduced to describe the data obtained in reactions induced by  $^{22}\text{Ne}$  and  $^{26}\text{Mg}$  (bottom panels).

ation in the LD fission barrier gives the calculated cross sections varied within a factor of 1.5 only (that is within the experimental errors). Such a weak sensitivity of the calculations for the heaviest nuclei is due to a relatively small LD component of the fission barrier (the main contribution is given by the shell correction energy  $\Delta W_{\text{gs}}$  in contrast to Fm–No nuclei, for which LD and shell components are comparable). This circumstance should be kept in mind in the analysis of reactions leading to still heavier nuclei. For the less asymmetric  $^{32}\text{S} + ^{238}\text{U}$  reaction,  $P_{\text{fus}} = 0.35$  can be derived from the analysis of capture and fusion cross sections obtained in fission experiments [8,35]. This value is comparable with  $P_{\text{fus}} = 0.16$  based on the 2.5 pb ER cross section obtained in  $^{238}\text{U}(^{34}\text{S}, 5n)^{267}\text{Hs}$  [36].

### 3 “Cold fusion” reactions

Applying the LD barriers obtained in the analysis of “hot fusion” reactions ( $k_f = 1.2$ ) to the production of Fm isotopes in the “cold fusion” reaction with  $^{40}\text{Ar}$ , one has to introduce again the empirical value of  $P_{\text{fus}} = 0.1$  to reproduce cross sections for  $^{40}\text{Ar} + ^{208}\text{Pb}$  [37]. The alternative independent fit to the data gives us significantly smaller LD fission barriers ( $k_f = 0.9$ ) that contradicts to the results of the analysis of the very asymmetric reaction

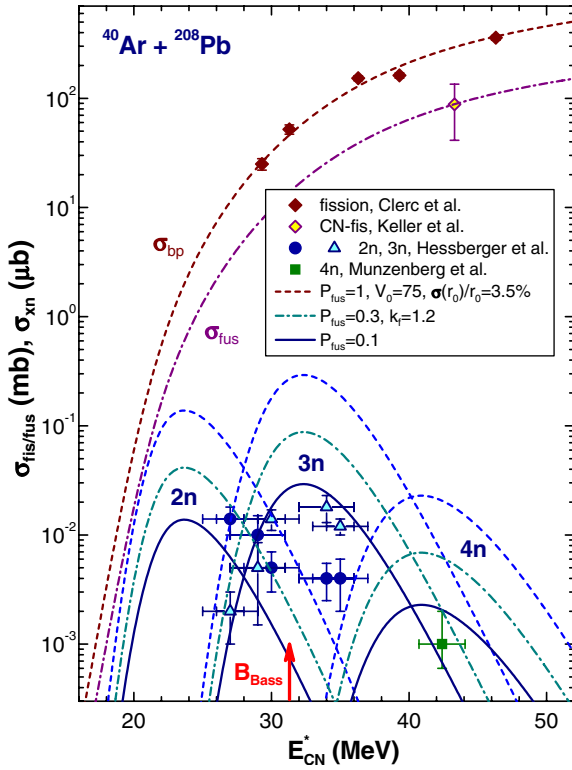


**Fig. 4.** (Color online) The same as in Figures 1–3, but for the cross sections data obtained for the  $^{40}\text{Ar} + ^{208}\text{Pb}$  reaction [37,38].

with  $^{16}\text{O}$ . The value of  $P_{\text{fus}} = 0.1$  is below the estimate of the CN-fission probability [38] (corresponding to  $P_{\text{fus}} \simeq 0.3$ ), which was obtained with the analysis of the fission-fragment charge-angular distributions (see Fig. 4). This estimate of the CN-fission contribution into the total capture-fission cross section was derived without any selections on the total kinetic energy of fission-like events and its variance, so it can be only considered as an upper limit for the value.

The analysis of the ER and fission cross section data compiled for the  $^{48}\text{Ca} + ^{208}\text{Pb}$  reaction [6,24,39,40] leads to the similar result as was obtained in the case of  $^{40}\text{Ar} + ^{208}\text{Pb}$ . Namely, the value of  $P_{\text{fus}} = 0.15$  was derived with the same LD fission barriers ( $k_f = 1.2$ ) that were obtained in the analysis of the C + Cm  $xn$  excitation functions corresponding to the No isotopes production [31]. Again, the alternative independent fit to the ER data gives us significantly smaller LD fission barriers ( $k_f = 0.8$ ) that contradicts to the results of the analysis of very asymmetric C + Cm reactions (see Fig. 5). Note that the fusion cross section restored with this approach is much lower than the experimental one corresponding to the symmetric mass division for fission fragments [6,40]. The same follows from the comparison of the “restored” cross section with the fusion one calculated in the framework of the two-center model [14]. At the same time, the “restored” cross section is noticeably higher than the one predicted with the model [41] based on the di-nuclear system concept.

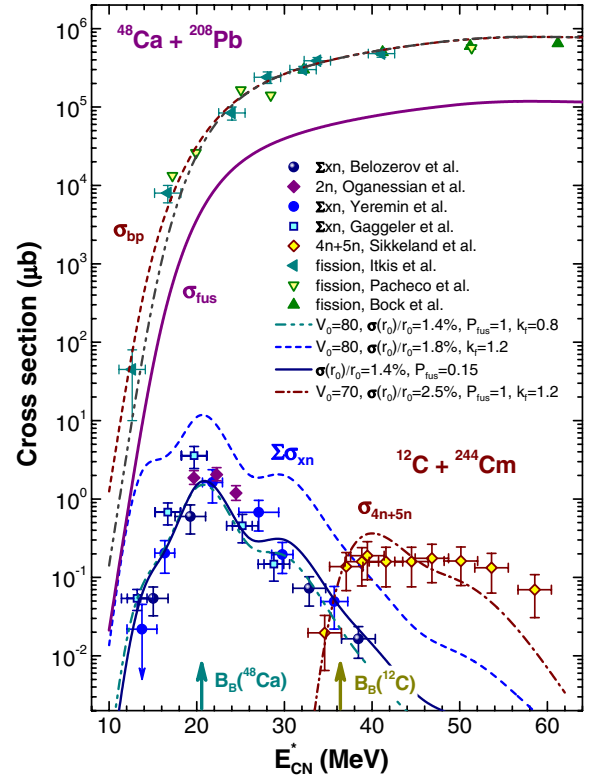


**Fig. 5.** (Color online) The same as in Figures 1–4, but for the reactions leading to  $^{256}\text{No}^*$ : for “cold fusion” in  $^{48}\text{Ca} + ^{208}\text{Pb}$  [6,24,39,40], the fusion cross section “restored” in calculations fitted to the ER data is shown; for “hot fusion” in  $^{12}\text{C} + ^{244}\text{Cm}$ , the ER cross sections [31] are displayed for a comparison.

Going to the  $^{50}\text{Ti}$  induced reactions leading to the production of neutron-deficient Rf and Db nuclei, one has to reduce strongly LD barriers, or to introduce empirically small values of the fusion probability in order to reproduce the  $xn$  cross section data [42]. Unfortunately, cross section data for the production of neutron-deficient Rf isotopes in asymmetric “hot fusion” reactions, which were obtained by Somerville et al. [32], can be reproduced within a factor 2 (the calculation is twice as large as the  $4n$  cross section and about the same factor as low as the  $5n$  one), if  $k_f = 1.0$  is used. Data for the production of the neutron-deficient Db isotopes in asymmetric “hot fusion” reactions are absent, so  $k_f = 1.0$  was used in both cases, bearing in mind a smooth variation in the LD component and possible isotopic effects following from the global parameterization of fission barriers [44]. It implies that the barrier heights reduce more strongly with decreasing neutron number, than the LD model predicts [19]. It is clear that if  $k_f$  increases,  $P_{\text{fus}}$  decreases and vice versa. The effect of the  $k_f$  scaling becomes negligible in the cases of the “cold fusion” reactions with  $^{54}\text{Cr}$  and  $^{58}\text{Fe}$  leading to Sg and Hs nuclei [2]. In the last case omitting a small LD component leads to a reduction of the ER cross section within a factor 2 only that is less sensitive than in the case of the calculations for “hot fusion” reactions. The results of the data analysis for the  $^{50}\text{Ti}$  and  $^{58}\text{Fe} + ^{208}\text{Pb}$  reactions are shown in Figure 6.

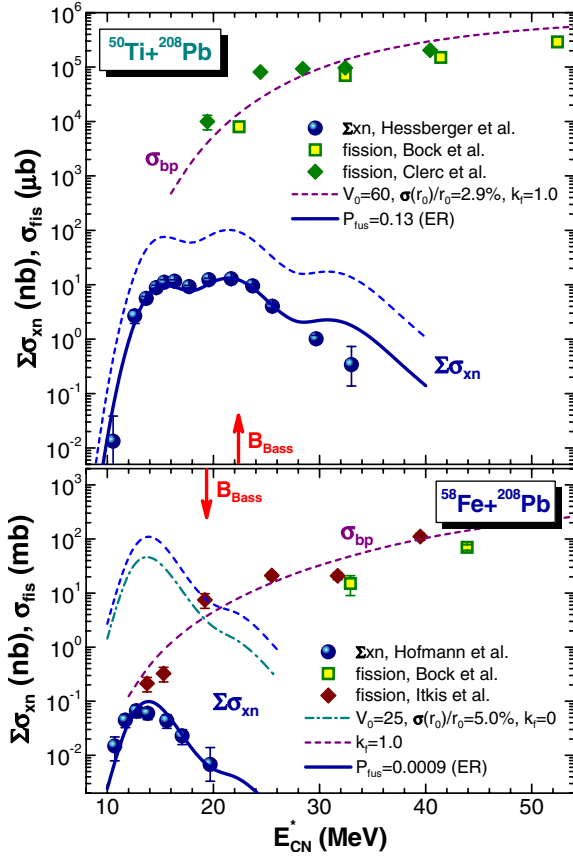


**Fig. 6.** (Color online) The same as in Figures 1–5, but for the cross sections data obtained for  $^{50}\text{Ti} + ^{208}\text{Pb}$  [2, 6, 42, 43].

Further analysis of more symmetric projectile-target combinations reveals that the barrier passing model (such as used in HIVAP) may not reproduce a very low capture cross section obtained in the  $^{64}\text{Ni} + ^{208}\text{Pb}$  reaction [6]. A decrease in the strength of the nuclear potential  $V_0$ , which helps in the description of the capture cross section lowering at the transition from  $^{48}\text{Ca}$  to  $^{58}\text{Fe}$ , is insufficient in the  $^{64}\text{Ni}$  case. Other forms of the nuclear potential could be checked for the description of the heaviest nuclei production in nearly symmetric combinations in the framework of the present barrier passing approach.

At the same time, it is reasonable to include in the analysis the ER data obtained in more asymmetric (“hot fusion”) combinations of Mg and S with Pb [39, 45]. The analysis of fission cross section data obtained in these reactions [6, 7] leads to  $P_{\text{fus}}$  values of 0.65 and 0.4, respectively. These values can be considered as upper limits for the fusion probability. Using  $k_f = 0.82$  obtained with the fit to fission and  $xn$  cross sections measured in the  $\alpha + ^{233}\text{U}$  reaction [46] (leading to more neutron-rich Pu isotopes than those obtained in  $^{24,26}\text{Mg} + ^{208}\text{Pb}$ ), one can estimate a low limit for  $P_{\text{fus}}$  for these reactions as  $\simeq 0.2$ . For the  $^{34}\text{S} + ^{207}\text{Pb}$  reaction  $P_{\text{fus}}$  is estimated to be 0.26, if the LD barriers corresponding to  $k_f = 1.0$  are used, as was obtained in the analysis of the  $^{12}\text{C} + \text{U}$  reactions leading to more neutron-rich Cf isotopes (see Fig. 1).

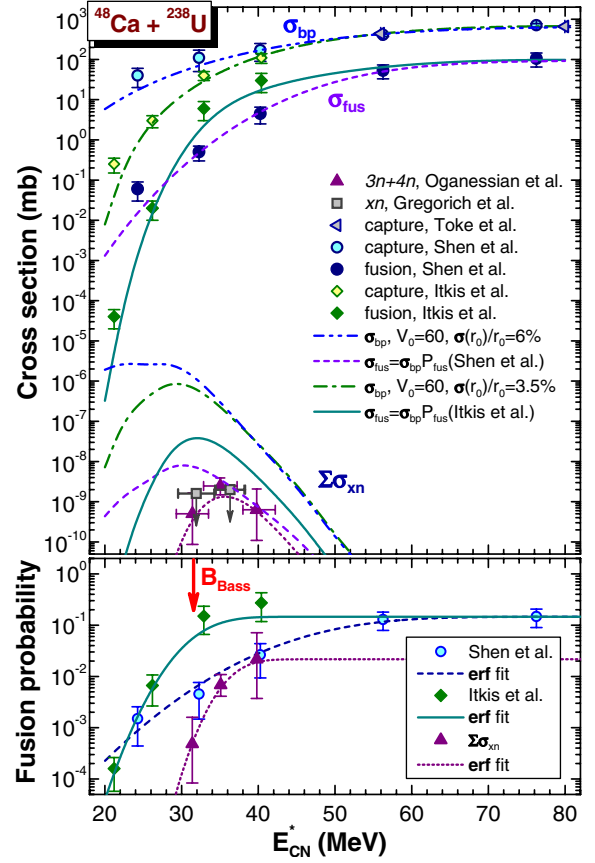


**Fig. 7.** (Color online) The same as in Figures 1–6, but for the cross sections data obtained for the  $^{48}\text{Ca} + ^{238}\text{U}$  reaction [5, 8, 40] (upper panel). The fusion probability functions derived with the analysis of the fission and  $\Sigma\sigma_{xn}$  data and their approximations with the error function are also shown (bottom panel).

#### 4 Reactions of $^{48}\text{Ca}$ with actinide target nuclei

A particular interest is an estimate of  $P_{\text{fus}}$  for reactions of  $^{48}\text{Ca}$  with actinide target nuclei, which lead to the formation of compound nuclei close to the island of stability of SHE with the center at  $Z = 114$  and  $N = 184$  (corresponding to the most stable closed shell nucleus). Survivability of such nuclei having a zero LD-barrier is mainly determined by the energies of shell corrections to the fission barriers. This circumstance simplifies the analysis, since one does not need to vary  $k_f$  at the LD barriers anymore. Bearing in mind the available data on fission [8, 40] and ER production [5], it is reasonable to chose the  $^{48}\text{Ca} + ^{238}\text{U}$  reaction as a starting point for the analysis (see Fig. 7).

Unfortunately, as one can see in Figure 7, the fission data sets are not in agreement with each other and require two different fusion probability functions that can be derived from the data [8, 40] instead of a single  $P_{\text{fus}}$  value. Applying these fusion probability functions to the barrier passing cross sections calculated with HIVAP one cannot reproduce the ER data. In fact, the ER excitation function calculated in this way (using the data [8]) extends

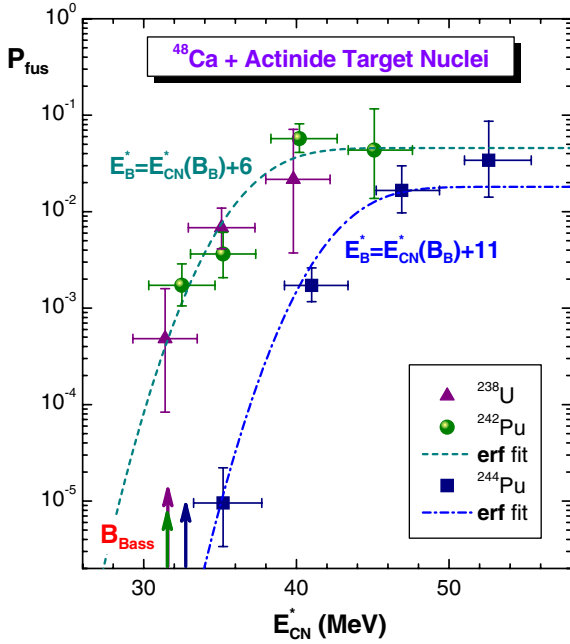


**Fig. 8.** (Color online) Fusion probability functions derived with the analysis of the  $\Sigma\sigma_{xn}$  data for  $^{48}\text{Ca} + ^{238}\text{U}$ ,  $^{242,244}\text{Pu}$  [5] (symbols) and their approximations with the error function (lines).

well below the nominal fusion barrier [23] that is not observed for the  $^{48}\text{Ca}$  ER data [5]. A fit to the fission data of Itkis et al. [40] leads to the calculated ER excitation function with the maximum position close to the one observed in the experiment, but with absolute cross sections much higher than those measured by Oganessian et al. [5]. One can derive the fusion probabilities as ratios of the sum of  $xn$  cross sections measured in [5] to the calculated ones at the same excitation energies and parameterize these values with an error function, as is shown in the bottom panel of Figure 7. A similar procedure was applied to the extraction of  $P_{\text{fus}}$  from the ER data obtained in nearly symmetric combinations of massive nuclei [9].

Attempting to generalize this approach, the  $xn$  cross section data obtained in the  $^{48}\text{Ca} + ^{242,244}\text{Pu}$  reactions [5] were also considered in a similar way as shown in Figure 8. The mean value of the fusion barrier  $E_B^*$  (expressed via the CN excitation energy), corresponding to a twofold decrease in  $P_{\text{fus}}$  (as compared with the asymptotic value at  $E_{\text{CN}}^* \gg E_B^*$ ), can be evaluated with the CN excitation energy at the Bass barrier  $E_{\text{CN}}^*(B_B)$  as  $E_B^* = E_{\text{CN}}^*(B_B) + \Delta E$ . A sizeable value of  $\Delta E = (6-11)$  MeV may reflect the effect of the nuclear deformation on a real fusion leading to the ER production in these reactions. Such shift of the fusion barrier relatively to the capture one, which is not observed in the “cold fusion” reactions, is similarly taken into account in the calculations of the ER production cross sections in  $^{48}\text{Ca}$  reactions with actinide target in the framework of two-center model approach [14].

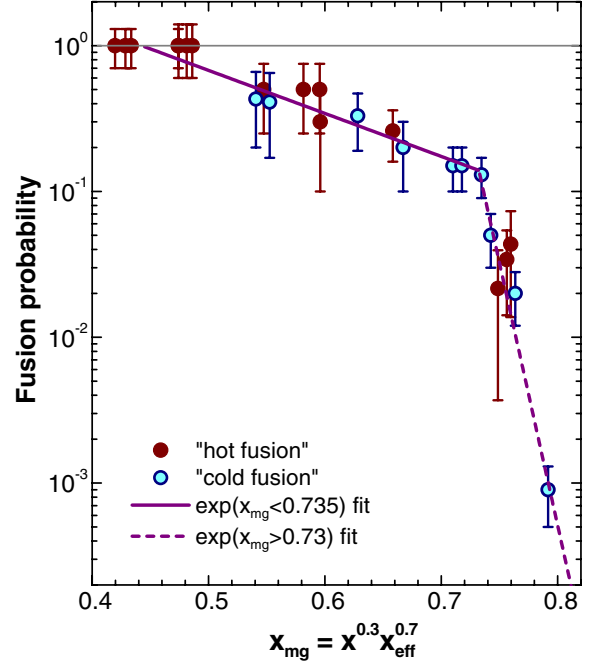


**Fig. 9.** (Color online) Fusion probability scaling derived with the combined fissility parameter [47] (symbols) and its approximations with the exponentials (lines).

## 5 Systematics of the fusion probability

The fusion probability values resulting from the analysis are in the range  $9 \times 10^{-4} \leq P_{\text{fus}} \leq 1.0$  (see the values in Figs. 3–6). As was mentioned, it was assumed that  $P_{\text{fus}} = 1.0$  for very asymmetric “hot fusion” reactions, such as those shown in Figures 1–3. In that cases errors in the values correspond to the (30–40)% accuracy declared in experiments. Similar errors were assigned to  $P_{\text{fus}}$  resulting from the analysis of “cold fusion” data. As was mentioned, in some cases (mainly due to uncertainties in  $k_f$ ) an upper limit in  $P_{\text{fus}}$  was determined from fission data, whereas a low limit corresponded to the maximal possible  $k_f$  value. All the  $P_{\text{fus}}$  values derived from the analysis are scaled with the combined fissility as shown in Figure 9. In search for scaling, the dependences of  $P_{\text{fus}}$  on the combined fissility  $x_{\text{ma}} = nx + (1-n)x_{\text{eff}}$  and  $x_{\text{mg}} = x^n x_{\text{eff}}^{1-n}$ , where  $x$  and  $x_{\text{eff}}$  are CN and effective fissility parameters [47], respectively ( $0 \leq n \leq 1$ ), were tested as was done in the case of the extra(-extra)-push energy scaling [6, 8, 47]. The best scaling was found for the  $P_{\text{fus}}$  dependence on  $x_{\text{mg}} = x^{0.3} x_{\text{eff}}^{0.7}$  for all the extracted fusion probability values. The values can be approximated with two exponentials as shown in Figure 9. Such scaling demonstrates a strong dependence of  $P_{\text{fus}}$  on the entrance channel (via the  $x_{\text{eff}}$  parameter), which is much stronger than those found for the extra(-extra)-push energy [6, 8, 47].

Some predictions of the production cross section can be done using the systematics with a view to choose the most effective reaction for the synthesis of a specific unknown nucleus, or to evaluate some reaction(s) unexplored yet for the synthesis of the heaviest elements. Thus the analysis shows that the best choice for the production of  $^{268}\text{Hs}$

is the  $^{232}\text{Th}(^{40}\text{Ar}, 4n)$  reaction, which gives the maximal production cross section at the level of (3–5) pb. Checking the ability to use projectiles heavier than  $^{48}\text{Ca}$ , one can evaluate the  $^{58}\text{Fe} + ^{238}\text{U}$  reaction leading to a neighbor CN with respect to the one produced in  $^{48}\text{Ca} + ^{249}\text{Cf}$ . In the last reaction, 3 atoms of the element 118 were recently observed in the  $3n$  reaction channel [48]. The reaction cross sections can be reproduced using  $P_{\text{fus}}$  given by the systematics with the fusion barrier corresponding to  $E_{\text{B}}^* = E_{\text{CN}}^*(B_{\text{B}}) + 7$  MeV. Fitting the capture cross section for  $^{58}\text{Fe} + ^{238}\text{U}$  [8] and taking  $P_{\text{fus}}$  from the systematics with the same fusion barrier parameterization, one can get a production cross section level below 1 fb for the most probable  $4n$  channel. Finally, a far extrapolation of the systematics gives us a very low fusion probability for the  $^{136}\text{Xe} + ^{136}\text{Xe}$  reaction ( $\approx 5 \times 10^{-8}$ ), which is partially compensated by a high survivability of ER. Both these factors lead to a production cross section at the level of 0.1 pb for the most probable  $1n$  evaporation channel.

## References

1. Yu.Ts. Oganessian, Lect. Notes in Phys. **33**, 221 (1974)
2. S. Hofmann, Rep. Prog. Phys. **61**, 639 (1998); S. Hofmann et al., Eur. Phys. J. A **14**, 147 (2002)
3. K. Morita et al., J. Phys. Soc. Jpn **73**, 2593 (2004)
4. A. Türler et al., Phys. Rev. C **57**, 1648 (1998); A. Türler et al., Eur. Phys. J. A **17**, 505 (2003); A. Türler, talk presented at *The III Sandanski Coordination Meeting on Nuclear Science*, Albena, 2005 (unpublished)
5. Yu.Ts. Oganessian et al., Phys. Rev. C **69**, 054607 (2004); Yu.Ts. Oganessian et al., Phys. Rev. C **70**, 064609 (2004)
6. R. Bock et al., Nucl. Phys. A **338**, 334 (1982)
7. M.B. Tsang et al., Phys. Rev. C **28**, 747 (1983); B.B. Back, Phys. Rev. C **31**, 2104 (1985); B.B. Back et al., Phys. Rev. C **32**, 195 (1985)
8. J. Töke et al., Nucl. Phys. A **440**, 327 (1985); W.O. Shen et al., Phys. Rev. C **36**, 115 (1987)
9. C.-C. Sahm et al., Nucl. Phys. A **441**, 316 (1985); A.B. Quint et al., Z. Phys. A **346**, 119 (1993)
10. A.C. Berriman et al., Nature **413**, 144 (2001); D.J. Hinde et al., J. Nucl. Radiochem. Sci. **3**, 31 (2002)
11. R.N. Sagaidak et al., Phys. Rev. C **68**, 014603 (2003)
12. G.G. Adamian et al., Phys. Rev. C **69**, 011601R (2004); G.G. Adamian et al., Phys. Rev. C **69**, 046401 (2004)
13. G. Fazio et al., Eur. Phys. J. A **19**, 89 (2004)
14. V.I. Zagrebaev, Phys. Rev. C **64**, 034606 (2001)
15. Caiwan Shen et al., Phys. Rev. C **66**, 061602R (2002)
16. Y. Aritomo, M. Ohta, Nucl. Phys. A **744**, 3 (2004)
17. W. Reisdorf, Z. Phys. A **300**, 227 (1981); W. Reisdorf, M. Schädel, Z. Phys. A **343**, 47 (1992)
18. R.N. Sagaidak et al., in *Proc. of the Intern. Conf. Nuclear Shells – 50 Years*, Dubna, 1999, edited by Yu.Ts. Oganessian, R. Kalpakchieva (WS, 2000), p. 199; R.N. Sagaidak et al., in *Proc. of the Intern. Workshop on Fusion Dynamics at the Extremes*, Dubna, 2000, edited by Yu.Ts. Oganessian, V.I. Zagrebaev (WS, 2001), p. 135; R.N. Sagaidak et al., in *Proc. of 10th Intern. Conf. on Nuclear Reaction Mechanisms*, Varenna, 2003, edited by E. Gadioli (Università di Milano, 2003), p. 301
19. S. Cohen et al., Ann. Phys. **82**, 557 (1974)
20. G. Audi et al., Nucl. Phys. A **729**, 337 (2003)
21. W.D. Myers, W.J. Swiatecki, Nucl. Phys. A **601**, 141 (1996); Report LBL-36803 (1994)
22. W. Reisdorf et al., Nucl. Phys. A **438**, 212 (1985)
23. R. Bass, Lect. Notes in Phys. **117**, 281 (1980)
24. H.W. Gäggeler et al., Nucl. Phys. A **502**, 561c (1989); A.V. Yeremin et al., JINR Rap. Com. **6**[92]-98, 21 (1998); A.V. Belozherov et al., Eur. Phys. J. A **16**, 447 (2003)
25. D.J. Hinde et al., Phys. Rev. C **53**, 1290 (1996)
26. T. Sikkeland et al., Phys. Rev. **169**, 100 (1968)
27. T. Murakami et al., Phys. Rev. C **34**, 1353 (1986); R. Vandenbosch et al., Phys. Rev. C **54**, R977 (1996); J.P. Lestone et al., Phys. Rev. C **56**, R2907 (1997)
28. Z. Liu et al., Phys. Rev. C **54**, 761 (1996)
29. G.N. Akapiev et al., Atom. Ener. **21**, 243 (1966) (*in Russian*); K. Nishio et al., JAERI-Review 2004-027, p. 39
30. M. Nurmia et al., Phys. Lett. **26B**, 78 (1967)
31. T. Sikkeland et al., Phys. Rev. **172**, 1232 (1968)
32. J.M. Nitschke et al., Nucl. Phys. A **352**, 138 (1981); L.P. Somerville et al., Phys. Rev. C **31**, 1801 (1985)
33. Yu.A. Lazarev et al., Phys. Rev. Lett. **73**, 624 (1994); M.R. Lane et al., Phys. Rev. C **53**, 2893 (1996); Yu.A. Lazarev et al., Phys. Rev. C **62**, 064307 (2000)
34. Y. Nagame et al., J. Nucl. Radiochem. Sci. **3**, 85 (2002)
35. R. Freifelder et al., Phys. Rev. C **35**, 2097 (1987)
36. Yu.A. Lazarev et al., Phys. Rev. Lett. **75**, 1903 (1995)
37. G. Münzenberg et al., Z. Phys. A **302**, 7 (1981); F.P. Heßberger et al., GSI Scientific Report 1986, GSI 87-1, p. 17; H.-G. Clerc et al., Nucl. Phys. A **419**, 571 (1984)
38. H. Keller et al., Z. Phys. A **326**, 313 (1987)
39. Yu.Ts. Oganessian et al., Phys. Rev. C **65**, 054602 (2002);
40. A.J. Pacheco et al., Phys. Rev. C **45**, 2861 (1992); M.G. Itkis et al., in *Proc. of the Intern. Workshop on Fusion Dynamics at the Extremes*, Dubna, 2000, edited by Yu.Ts. Oganessian, V.I. Zagrebaev (WS, 2001), p. 93
41. G. Fazio et al., Mod. Phys. Lett. A **20**, 391 (2005)
42. F.P. Heßberger et al., Z. Phys. A **359**, 415 (1997); F.P. Heßberger et al., Eur. Phys. J. A **12**, 57 (2001)
43. H.-G. Clerc et al., Nucl. Phys. A **419**, 571 (1984)
44. M. Dahlinger et al., Nucl. Phys. A **376**, 94 (1982)
45. A.N. Andreyev et al., Z. Phys. A **337**, 231 (1990); A.N. Andreyev et al., Z. Phys. A **347**, 225 (1994)
46. R. Vandenbosch et al., Phys. Rev. **111**, 1358 (1958); J.R. Huizenga et al., Phys. Rev. **124**, 1964 (1961); H. Delagrange et al., Phys. Rev. C **17**, 1706 (1978)
47. J.P. Blocki et al., Nucl. Phys. A **459**, 145 (1986)
48. Yu.Ts. Oganessian et al., Phys. Rev. C **74**, 044602 (2006)